Counting the Number of Glutamate Molecules in Single Synaptic Vesicles

Yuanmo Wang,[†] Hoda Fathali,[†] Devesh Mishra,[‡,⊥] Thomas Olsson,[∥] Jacqueline D. Keighron[#], Karolina P. Skibicka,[⊥,‡] and Ann-Sofie Cans*[,†]

[†]Department of Chemistry and Chemical Engineering, Chalmers University of Technology, Kemigården 4, SE-412 96 Gothenburg, Sweden;

[‡]Department of Physiology/Metabolic Physiology, Institute of Neuroscience and Physiology, The Sahlgrenska Academy at the University of Gothenburg, Medicinaregatan 11, SE-413 90 Gothenburg, Sweden;

[#]Department of Chemical and Biological Sciences, New York Institute of Technology, Old Westbury, NY 11568, USA

[∥]Department of Physics, Chalmers University of Technology, Kemigården 4, SE-412 96 Gothenburg, Sweden;

[⊥] Wallenberg Centre for Molecular and Translational Medicine, University of Gothenburg, SE-405 30 Gothenburg, Sweden

Corresponding author email address:

* cans@chalmers.se

Table of Content

I. Experimental Procedure

Materials. 5U L-Glutamate Oxidase (GluOx) lyophilized powder from *Streptomyces sp*., sodium chloride (NaCl), sodium bicarbonate ($NaHCO_3$), gold chloride trihydrate ($HAuCl_4$), ferrocene-methanol (FcMeOH), Whatman® Anotop® 25 syringe filters with 20 nm filtering size, phosphate-buffered saline (PBS) tablets (10 mM, pH 7.2), sulfuric acid (H_2SO_4), copper sulfate ($CuSO_4$), monosodium glutamate, glycerol, potassium chloride (KCl), monosodium phosphate (anhydrous, NaH_2PO_4), calcium chloride ($CaCl_2$), magnesium chloride ($MgCl_2$), magnesium sulfate ($MgSO_4$), Adenosine 5′-triphosphate (ATP), cOmplete (EDTA-free) tablets, glucose, tungsten wire, HEPES and sucrose were purchased from Sigma-Aldrich (St. Louis, MO, USA). 1,2-dioleoyl-sn-glycero-3-phosphocholine (DOPC), 1,2-dioleoyl-sn-glycero-3-phosphoethanolamine (DOPE) and cholesterol were purchased from Avanti Polar Lipids Inc., USA. MilliQ water with resistivity ≥ 18 MΩ.cm was used in all experiments.

Preparation of glutamate-filled LUVs. Lipid vesicles were prepared by mixing DOPC, DOPE and cholesterol in mass ratio 50:25:25 to achieve molar ratio 39:21:40. The flask containing mixed lipids was rotoevaporated under N_2 for three hours to eliminate the chloroform used for dissolving the lipids and to form a thin lipid film at the surface of the glass rotoevaporation flask at vacuum condition. The lipid vesicles were formed by rehydrating the thin lipid film with glutamate buffer solution during an incubation of 30 min at room temperature. The total lipid concentrations were approximate 2.5 mg/ml after the dehydration process. To entrap a homogenous glutamate solution inside the lipid vesicles, Falcon tubes containing rehydrated lipid vesicle solution was alternately placed into liquid nitrogen and room temperature water to create five freeze-thaw cycles.[15] To unify the vesicle size, the lipid vesicle suspension was extruded through a 400 nm pore sized polycarbonate membrane (Whatman, USA) 21 times using Avanti Mini-Extruder (Avanti Polar Lipids, Inc., USA) under the same pressure (i.e. 1 bar) generated by N_2 gas at room temperature. Illustra™ Microspin™ S-200 HR columns (GE Healthcare, Buckinghamshire, UK.) were used to remove the non-loaded glutamate from the vesicle suspension. The collected glutamate lipid vesicle solution was used immediately in experiments within 4 hours of synthesis and stored at 4 ℃ during waiting time.

Glutamate loading buffer were prepared by dissolving monosodium glutamate into 10 mM HEPES with pH 7.4 at different concentrations as follows: 100 mM with osmotic pressure 156 mOsm/kg, 150 mM with 262 mOsm/kg, 200 mM with 343 mOsm/kg, 250 mM with 421 mOsm/kg and 300 mM with 496 mOsm/kg. The dilution buffer needed for electrochemical and vesicle size measurements were made by dissolving NaCl into 10 mM HEPES with pH 7.4, the osmotic pressure of dilution solution in 10 mM HEPES (pH 7.4) was adjusted by NaCl to a same value that matches the corresponding glutamate concentration that was used for loading the vesicles.

Size measurements of glutamate of LUVs. The size distribution of glutamate lipid vesicles was measured using Nanoparticle Tracking Analysis (NTA) system (NanoSight LM10, Malvern Instruments Ltd, UK). For each vesicle batch the sample was first run at 2000 x dilution using the osmotic pressure-controlled dilution buffer to determine the vesicle concentration; based on the outcome, the sample dilution was then adjusted to match the optimal concentration for measurement by the instrument. All measurements were done at a constant temperature (25 °C) using a module and for each sample, five measurements were recorded for a period of 1 minute, during flow condition (to increase number of particles tracked). All size measurements were carried out immediately after lipid vesicles preparation.

Fabrication of an ultrafast glutamate sensor. Carbon fiber microelectrodes were made by aspirating single 33 μm in diameter carbon fibers into borosilicate glass capillaries (1.2 mm outer diameter, 0.69 mm inner diameter, Sutter Instrument Co., Novato, CA, USA). The capillaries with a carbon fiber inserted on the inside were then pulled from the using a micropipette puller (model P-1000, Sutter Instrument Co., Novato, USA) to created two tapered glass-coated carbon fiber tip electrodes. To seal the glass-carbon fiber junction of the electrode, the electrode tips were placed into epoxy solutions (EpoTek 301, Epoxy Technology, Billerica, MA, USA) for 2 minutes and thereafter incubated in the oven at 100 ℃ overnight. The electrode tips were then cut near the carbon-glass junction under microscope using a scalpel and were thereafter polished at a 45° angle using a micropipette beveller (model BV-10, Sutter Instrument Co., Novato, USA) to achieve a glass-coated insulated disc electrode surface. Prior to further modifying the electrode tip surface, the electrodes were backfilled with 3M KCl solution and a tungsten wire were used to connect the electrode to a an electrical head stage to test the electrode performance in a 1 mM FcMeOH solution by performing cyclic voltammetry and scanning the voltage between -0.2 V and +0.8 V against a saturated Ag/AgCl reference electrode (CH Instruments, USA) at 0.1 Vs^{-1} using a potentiostat (model 650A Series Multi-Potentiostat, CH Instruments, USA). Only electrodes with a stable steady-state current and expected current size amplitude were used.

Gold nanoparticle (AuNP) hemispheres were electrochemically deposited onto the electrode tip surface in a similar way to the method of Finot et. al. [16] with minor alterations as performed in our lab [12]. Briefly here, the carbon working

electrode and an Ag/AgCl reference electrode were immersed into 0.5 mM $HAuCl_4$ solution, a potential of +1.2 V was applied to the carbon electrode surface for 10 s followed by switching the potential down to -0.6 V for 24 s via the 650A Series Multi-Potentiostat (CH Instruments, USA). The AuNP surface area was examined electrochemically by applying potential onto the AuNP-coated carbon electrode against a $Cu/CuSO_4$ reference electrode via a linear sweep from +1.4 V (held for 5 s) to +0.5 V at a rate of 0.1 Vs^{-1} in 500 mM H_2SO_4 [12]. The charge of deposited AuNP was determined by integrating the resulting peak at around +0.8 V and the obtained charge was divided with a constant derived from the Finot method that was equal to 489 μC cm^{-2}.[16]

At the last step of the glutamate sensor fabrication, an ultra-thin layer of enzyme was immobilized onto the AuNP-coated carbon electrode using the protocol developed from our lab that control the enzyme layer thickness to a monolayer. [11] To completely dissolve the enzymes used for coating the electrode, 500 μL of 10 mM sodium bicarbonate (pH 8.2) was added into the L-Glutamate Oxidase lyophilized powder bottle (5U) and allowed the enzyme to dissolve by gently rotate the bottle. GluOx was allowed to self-adsorb onto the sensor surface by immersing the AuNP-coated electrode tip into 100 μl freshly prepared enzyme solution for approximate 2-3 hours at room temperature. The glutamate sensors were immediately used after fabrication, or otherwise stored in 10 mM PBS (pH 7.2) at 4 °C before use within 6 hours.

Mouse and rat brain slice preparation. Rodent brain slices were prepared from the brain of 4 - 8 weeks old male mice (C57BL) and rats (Sprague Dawley) that were purchased from Charles River, Sulzfeld, German. The rodents were group housed in a 12-h light/dark cycle with 0700 hours light on and supplied with *ad libitum* chow (Teklad Global 16% Protein Rodent Diet 2016, Envigo, Huntingdon, UK) and water. The animal experiments were performed in accordance with the Swedish Animal Welfare law and the local ethical committee regulations for animal research with ethics number 29-2014 at the University of Gothenburg, Sweden. Before decapitation, they were anesthetized using isoflurane (Baxter Medical AB, Sweden), brains were quickly removed and cut into 400 μm slices using Microtome HM 650 V (Thermo Fisher Scientific, Loughborough, UK) in 3 °C glycerol solution containing: 11 mM glucose, 7 mM $MgCl_2$, 1.2 mM $CaCl_2$, 2.5 mM KCl, 25 mM $NaHCO_3$, 1.2 mM NaH_2PO_4 and 219 mM glycerol. Coronal slices containing nucleus accumbens were incubated in medium containing 15 mM sucrose, 4 mM $MgCl_2$, 10 mM D-Glucose, 1 mM $CaCl_2$, 25 mM $NaHCO_3$, 1.25 mM NaH_2PO_4, 2.5 mM KCl, 125 mM NaCl for at least 45 min at 30 °C, and then transferred into a microscope-associated submerged chamber filled with artificial cerebrospinal fluid (aCSF) solution at a flow rate of 1 ml min^{-1} at room temperature. aCSF solution containing 2 mM $CaCl_2$, 25 mM $NaHCO_3$, 2.5 mM KCl, 125 mM NaCl, 10 mM D-Glucose 10 and 1.3 mM $MgCl_2$ were aerated with mixture of 5% carbon dioxide and 95% oxygen for at least 30 min before putting in brain slice and aeration was continued during the whole recording process.

Preparation of isolated synaptic vesicle. Synaptic vesicles were isolated from the same fresh mice brain that were used in the brain slice experiment. The work was performed with protocol that was summarized by the group of Jahn lab[17] and the group of Chiu lab[18] with slightly modification. Briefly, a whole brain was removed from one decapitated mouse and washed in ice-cold homogenization buffer containing 10 mM HEPES, 300 mM sucrose, 4 mM KCl, 4 mM $MgSO_4$ with freshly added 4 mM ATP and protease inhibitors cOmplete, pH 7.4. The collected brain was homogenized in ice-cold homogenization buffer with 10 strokes at 900 r.p.m. using a glass-Teflon homogenizer, followed by centrifuging the homogenization mixture at 1000g at 4 °C for 10 min. The collected supernatant (S1) was continuously centrifuged at 15000g and 4 °C for 15 min, the supernatant (S2) in this round was taken out and stored on ice. The left pellet (P2) was homogenized at 2000 r.p.m. with three strokes after adding 9 ml ice-cold homogenization buffer and centrifuged at 17000g for 15 min at 4 °C, the supernatant (LS1) was again collected and mixed with S2. The LS1/S2 mixture was centrifuged at 48000g for 25 min at 4 °C and collected the supernatant (CS1) that contain isolated glutamate synaptic vesicles. All high-speed centrifugation was performed using an ultracentrifuge (L-80, Beckman Coulter Inc., Indianapolis, IN, USA). CS1 solution was used for later electrochemical measurements.

Electrochemical measurements of glutamate content in glutamate-filled lipid vesicles. Prior to amperometric measurements of glutamate in synthetically prepared glutamate-filled lipid vesicles, the functionality of each glutamate sensors was tested in 100 mM glutamate solution (dissolved in 10 mM HEPES with pH 7.4) by performing cyclic voltammetry that scans the potential on glutamate sensor between -0.2 V and +0.8 V versus a chlorinated Ag wire as reference electrode at 0.1 Vs-1 using a HEKA patch clamp amplifier (EPC 10, HEKA elektronik, Lambrecht, Germany), only sensors that gave a response of a correct estimated current amplitude for the reduction of hydrogen peroxide, which serve as the reporter molecule for glutamate were used. The glutamate-filled lipid vesicles were diluted about 2 to 5 times with the same dilution solution used for NTA measurements before electrochemical measurements to ensure vesicle rupture to be initiated. The amperometric recordings were performed by holding potential onto sensor at 0 mV for 15 s and switched down to a constant potential for a 3-5 min recording time (i.e. -500 mV, -700 mV and -900 mV)

versus a Ag/AgCl reference electrode that was placed in the lipid vesicle solution using a patch clamp amplifier (Axopatch 200B, Molecule Devices, Sunnyvale, CA, USA) with a low-noise data acquisition system Axon™ Digidata® 1550B (Molecule Devices, Sunnyvale, CA, USA). The data were sampled at room temperature and at 20 kHz with an internal low pass Bessel filter at 2 kHz. The scaled output was set to 0.5 mV/pA.

Electrochemical measurements of glutamate exocytotic activity in rodent brain slice. The glutamate sensors were tested by chronoamperometry before performing *ex vivo* amperometric recordings of spontaneous exocytosis activity, by placement into 100 mM glutamate bulk solution (dissolved in aCSF) and applied on a constant potential of 0 V for 10 s followed by a potential switch to -0.5 V for 1 min (versus a Ag/AgCl disc reference electrode) using a patch clamp amplifier (MultiClamp 700B, Molecule Devices, Sunnyvale, CA, USA). Only sensors which provided a steady-steady state current amplitude corresponding to the glutamate concentrations in solution were used for experiments. With a 45° beveled electrode angle, the sensor tip was placed at the NAc region of coronal planes that contain glutamatergic terminals from various brain regions with the assistance of an upright Nikon E600FN (Nikon Inc., Japan) fluorescence microscope mounted with 4× lens, and by placement of the sensor in the brain slice using methods as previously published. [11] The amperometric recordings were carried out by applying a constant potential of -0.5 V to the sensor surface versus a Ag/AgCl disc reference electrode, using the same MultiClamp 700B. Except for two measurements that were recorded using a digitizer (model Digidata 1440A, Molecule Devices, Sunnyvale, CA, USA) at 10 kHz and filtered at 4 kHz using the internal low pass 4-pole Bessel filter, all the other measurements were sampled at 20 kHz and filtered at 10 kHz. Scaled output factor was 0.5 mV/pA.

Electrochemical measurements of glutamate in isolated synaptic vesicles. Before performing amperometric measurements of isolated glutamate synaptic vesicles, the glutamate sensors were tested in the same way as when used in brain slice experiments. CS1 solution were diluted 10 times before measurements using homogenization buffer. Amperometric measurements were performed by holding 0 mV onto sensor surface versus a Ag/AgCl disc reference electrode for 10 s, followed by lowering the potential to -0.5 V for 5-10 min using a patch clamp amplifier (MultiClamp 700B) at room temperature. Control experiments were performed similarly using pure homogenization buffer solution. All measurements were recorded at 20 kHz and filtered at 10 kHz using an internal low pass Bessel filter. Scaled output was adjusted to 0.5 mV/pA as well.

Analysis of amperometric data. All amperometric data were analyzed with IgorPro 6.37 software (WaveMetrics, Lake Oswego, OR, USA) using an Igor Procedure File for single spike events developed by David Sulzer's group [19]. The data were smoothed down to 5 kHz (binomial sm.), spikes were the current spikes detected exceed 5 times the signal of the standard deviation of the derivative of background current noise with respect to time. All traces were carefully checked and false-positive spikes were manually removed. Only current traces containing more than 30 spikes were used in the analysis. Different current spike parameters were defined as follows: T_{rise} and T_{fall} are rise and fall time between 25% and 75% of a peak signal, $T_{1/2}$ is the time of half maximum of a peak, I_{max} is the highest current of a peak, Q is the charge detected in each peak.

II. Additional Data

In this supportive information we present additional data from the process of characterizing this new amperometric method for quantitative analysis of glutamate content in single synaptic vesicles using an ultrafast enzyme-based glutamate sensor. In addition, we characterized this method for quantitative analysis of rapid transients of glutamate release at single exocytosis events in brain tissue.

The applied potential and the LUV glutamate concentration affect vesicle rupture frequency.

To better understand what drives vesicles to rupture at the glutamate sensor surface and to characterize the experimental conditions for valid quantitative glutamate measurement in these applications, we first investigated the effect of applied potential on vesicles rupture frequency at the glutamate sensor surface. For this, we prepared samples of LUVs that were pre-filled with various concentrations of glutamate solution (100, 150, 200, 250, 300 mM) and then used our ultrafast glutamate sensor to probe the LUV glutamate content, while varying the applied potential from -0.5 to -0.7 V and -0.9 V (vs a Ag/AgCl reference electrode) at the sensor surface.

From these recordings, the average frequency of vesicle rupture events was determined both as a function of the applied potential and versus the glutamate concentration used for loading the LUVs and was measured at time intervals of 5, 25, 45 and 65 s from the initial start of the amperometric recordings. As summarized in Table S1 A, B, the results from this analysis showed that the applied electric field at the sensor surface has a direct impact, where a larger amplitude of the negative potential applied enhances vesicle rupture. This is similar to previous observations for carbon fiber amperometry analysis of catecholamine-containing vesicles, where a larger positive potential trigger vesicles to more frequently rupture at the electrode surface.[1] Prevailing theory states that by increasing the potential the higher energy of the electric field created at the electrode surface, destabilizes the membrane of the vesicles that are adsorbed at the electrode surface, as vesicles often deform in response to the applied electric field, which facilitates formation transient pore forming across the vesicle membrane.[2] These membrane pores are not stable and may either close or that the pore dilates to a larger size, if an the pore line tension reach a sufficient high energetic cost that vesicles fully break open.[3,4] Taken together with our experiments on characterizing glutamate-containing vesicles, shows that it is not a matter of polarity, but rather the magnitude of the applied potential that is key. This is in line with the mechanism for electroporation that a larger electric field assists likelihood of pore formation in lipid membranes. As the electric field quickly loses its strength from the surface and into the physiological sample solution, vesicles need to be in close proximity to the electrode surface for the membrane to respond to the applied potential. Hence, a crucial aspect for the method to be valid for quantification of glutamate-containing vesicles is the design of our glutamate sensor. In contrast to conventional enzyme-based glutamate sensors where thicker layers of GluOx usually are immobilized to the sensor surface, our sensor is constructed with an ultra-thin enzyme coating. The enzyme layer is limited to the thickness of an enzyme molecular monolayer, which means that vesicles may come up to a few nanometers away from the electrode surface considering an estimated diameter of GluOx is about 7 nm, assumed by considering its molecular weight.

In addition to this finding, we found that the concentration of the encapsulating glutamate solution also played a role in facilitating vesicle rupture. For the 5 concentrations of glutamate tested, we found that a 200 mM glutamate solution had a 2- to 7-fold larger vesicle rupture activity than LUVs encapsulating a lower (100, 150 mM) or higher (250, 300 mM) glutamate concentration while applying a constant potential to the electrode surface independent of the amplitude of applied potential (Table S1A,B). This suggests that the encapsulation of glutamate solution into the LUVs significantly affect the vesicle membrane properties and its physical response to the applied electric field. Glutamate is one of the neurotransmitters known to bind lipid membranes and is also thought to partition into membrane to interact with the lipid head groups.[5] This molecular interaction that is mainly electrostatic involve interaction with the inner leaflet of the lipid bilayer, and the glutamate molecules can cause structural rearrangements of lipids membrane, which alters the density of lipid packing. This can significantly alter the vesicle membrane permeability and elastic properties which are factors known to affect both vesicle adsorption and electroporation efficiency and hence can modify the vesicle´s ability to rupture at the sensor surface.[3,5–10]

Table S1 (A). Frequency (Hz) of vesicle rupture as a function of the applied potential and concentration of glutamate solution used for loading the LUVs.

Applied potential (mV)	Concentration of glutamate loaded (mM)	Time after initiating the amperometric measurement (Hz)			
		5s	25s	45s	65s
-500	100 (n = 4)	8±3	5±3	4±3	2.7±0.8
	150 (n = 4)	2.7±0.7	5.0±0.6	6±1	6±1
	200 (n = 4)	18±11	21±5	12±4	28±8
	250 (n = 5)	4±1	2.2±0.8	3±1	3±1
	300 (n = 4)	3.9±0.9	2.9±0.4	4.4±0.7	2±1
-700	100 (n = 4)	16±6	16±8	11±7	13±4
	150 (n = 4)	15±2	23±4	26±5	18±4
	200 (n = 4)	41±5	70±10	59±8	48±4
	250 (n = 4)	16±3	19±2	14±2	19±2
	300 (n = 4)	11±1	20±4	19±3	11±3
-900	100 (n = 4)	18±2	23±2	28±6	27±2
	150 (n = 4)	50±11	36±13	39±14	44±13
	200 (n = 4)	100±29	61±11	73±22	80±15
	250 (n = 4)	39±5	41±8	32±6	36±9
	300 (n = 4)	22±5	31±8	24±1	23±3

The data is presented as the mean frequency ± SEM.

Table S1 (B). Frequency (Hz) of vesicle rupture as a function of applied potential and concentration of glutamate solution used for loading LUVs, where each frequency value represent the average frequency for the first 65 s of recording time and for each concentration of glutamate solution used to pre-fill the LUVs, as listed in Table S2 (A).

Applied potential (mV)	Concentration of glutamate loaded (mM)				
	100 mM	150 mM	200 mM	250 mM	300 mM
-500 (n=4)	5±1	4.8±0.7	20±7	2.7±0.5	3.3±0.5
-700 (n=4)	14±6	20±5	54±5	17±2	15±2
-900 (n=4)	24±2	42±10	78±8	37±6	25±2

The data are shown as the average of frequency at 5 different loaded concentrations ± SEM.

The mechanism for vesicle rupture and content release are not affected by the applied sensor potential or the concentration of the encapsulating glutamate solution.

After we found that the applied potential and the encapsulated glutamate concentration affected the mechanism for vesicle glutamate release through mediated electroporation at the sensor surface, we also studied the kinetic parameters of the recorded current spikes that were collected from the recording of glutamate release from glutamate-filled LUVs. The parameters extracted from each recorded current spike are as defined in the schematic in Figure S1A, which demonstrates a typical amperometric current spike detected in these measurements. In this analysis, we first examined the parameters featuring the temporal components such as the spike rise time (T_{rise}) that is marked as the time it takes for the peak current to rise from 25% to 75% of its maximum amplitude (I_{max}), the spike fall-time (T_{fall}) measuring the time for current drop from 75% to 25% of I_{max} and the current spike half-time ($T_{1/2}$) defined as the width of the spike at half-maximum amplitude. Here, T_{rise} is thought to be related to the detection of glutamate released from the time the initial pore that is formed due to electroporation and is large enough for glutamate to escape and the glutamate that continuously is released through a pore the continues to dilate and finally leads to shattering of the organelle and the full vesicle glutamate content is released. Finally, the parameter T_{fall} is thought to be connected to the time that it takes for neurotransmitters to diffuse from the release site to the electrode surface for detection and $T_{1/2}$ is the timing of the event. As shown in Figure S1 B-D, it was evident that the spike kinetic parameters $T_{1/2}$, T_{rise} and T_{fall} were not affected by either the amplitude of the applied potential or the glutamate concentration encapsulated inside the LUVs. This suggests that once the initiate pore has been formed in vesicle membrane, it is the same mechanisms affecting the vesicle pore to dilate and rupture the vesicle, without significantly affecting the rate of the pore dilation and glutamate release from the vesicle compartment or its rate for detection at the electrode surface.

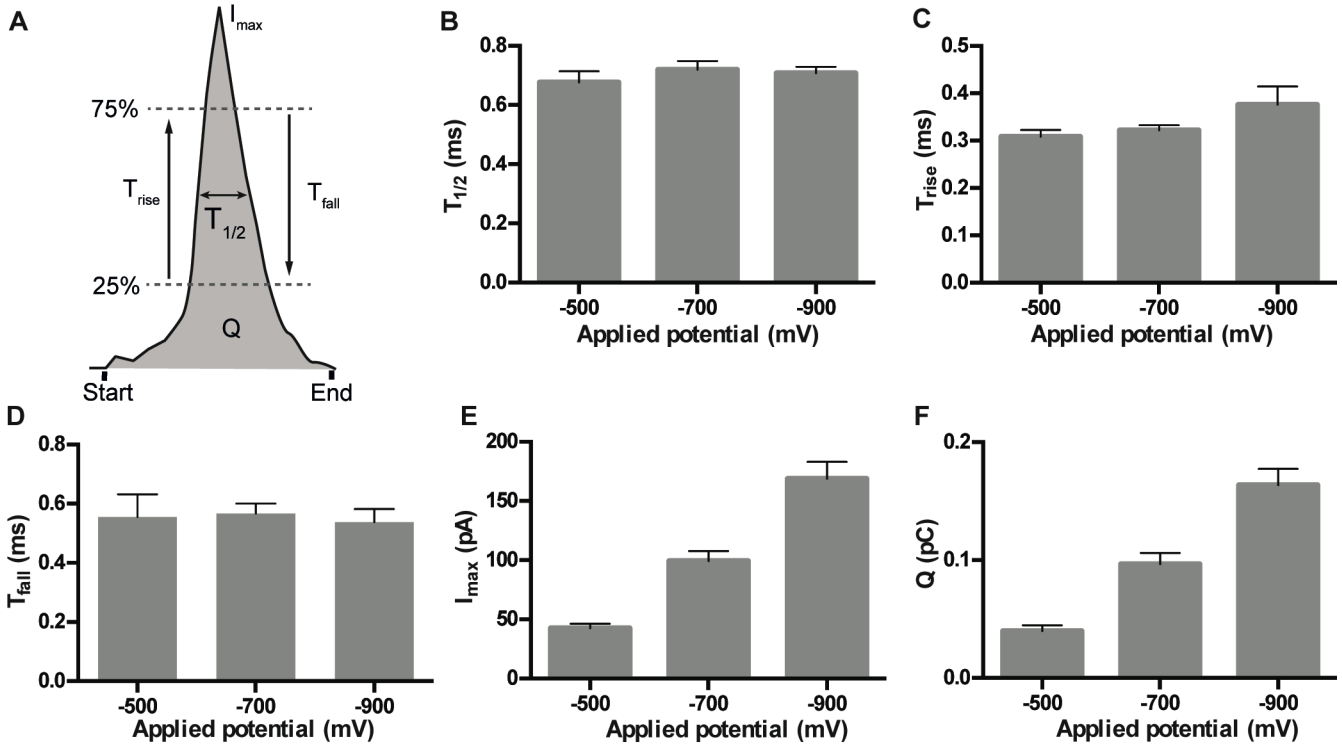

Figure S1. Analysis of the effect of the applied potential on the current spike kinetic and quantitative parameters at amperometric recording of glutamate release from glutamate-filled LUVs. (A) The definitions of the current spike parameters used for analysis. The applied potential effect on (B) spike rise-time (C) spike fall-time (D) spike half-width (E) the maximal current amplitude (F) the total integrated current spike charge. The data are shown as the means of spike kinetics from 5 different glutamate concentrations loaded into LUVs ± SEM.

Current spike amplitude and total charge increases with potentials applied.

The quantitative features I_{max} and the total integrated charge (Q) of the current spikes detected (Figure S1A) from the recording of LUV glutamate release were then analyzed as the function of applied potential and concentration of encapsulated glutamate solution. The total charge from a single current spike is directly related to the mole of analytes, N, that reach the electrode for detection and therefore the number of molecules that reach the electrode surface for detection can be calculated through Faraday´s law ($Q = nNF$) where, n is the number of electrons involved for the reduction reaction ($n = 2$ electrons gained for the reduction reaction of H_2O_2) and F is Faradays constant (96 485 C/mol). Hence, through the division of N by Avogadro´s number (6.022×10^{23} mol^{-1}), the number of H_2O_2 molecules detected by the electrode from a single vesicle release event can then be calculated. We observed in these measurements that both I_{max} and Q increased with a more concentrated encapsulated glutamate concentration in the LUVs and were also significantly affected by the magnitude of the applied potential (Table S2 and Figure S1E,F). This is in agreement with the cyclic voltammograms for the glutamate sensor,[11,12] which show an increase in current amplitude with change in applied potential from -0.5 V to -0.7 and -0.9 V.

Table S2. Analysis of current spike parameters as a function of the applied potential at the glutamate sensor surface when performing amperometric recording of glutamate release from LUVs pre-filled with various concentrations of glutamate solution.

Applied potential (mV)	Concentration of glutamate loaded (mM)	$T_{1/2}$ (ms)	T_{rise} (ms)	T_{fall} (ms)	I_{max} (pA)	Q (fC)	Spike No.
-500	100 (n = 4)	0.63±0.05	0.30±0.03	0.41±0.06	34±5	27±5	509
	150 (n = 4)	0.69±0.06	0.33±0.01	0.53±0.04	35±3	30±2	832
	200 (n = 4)	0.59±0.04	0.27±0.02	0.41±0.05	54±4	40±2	747
	250 (n = 5)	0.8±0.1	0.35±0.03	0.8±0.2	44±8	50±6	356
	300 (n = 4)	0.66±0.07	0.29±0.03	0.6±0.1	47±4	51±1	523
-700	100 (n = 5)	0.74±0.04	0.34±0.03	0.51±0.03	77±4	73±2	628
	150 (n = 4)	0.74±0.09	0.34±0.06	0.5±0.1	88±17	73±3	948
	200 (n = 4)	0.69±0.04	0.29±0.02	0.55±0.04	104±7	104±5	460
	250 (n = 4)	0.70±0.06	0.30±0.03	0.58±0.07	125±25	115±9	448
	300 (n = 4)	0.79±0.09	0.34±0.01	0.7±0.1	98±10	117±12	369
-900	100 (n = 4)	0.65±0.06	0.31±0.07	0.52±0.02	131±30	127±26	466
	150 (n = 4)	0.74±0.04	0.5±0.1	0.51±0.03	145±26	137±16	950
	200 (n = 4)	0.67±0.02	0.36±0.02	0.40±0.01	201±14	170±12	1260
	250 (n = 4)	0.72±0.08	0.30±0.04	0.65±0.09	202±37	200±30	848
	300 (n = 4)	0.76±0.07	0.41±0.08	0.6±0.1	165±24	185±7	441

The data are presented as the average of means ± standard error of the mean (SEM).

Using glutamate-filled LUVs to calibrate quantitative vesicle glutamate measurements

Biosensors need calibration to translate the electrical signal recorded into analyte concentration. It is important that the calibration is designed with matching experimental conditions as used for the quantitative measurements. Therefore, we introduced a calibration method for glutamate synaptic vesicle analysis based on probing glutamate release from LUVs that were pre-filled with various glutamate concentrations when performing the glutamate measurement at a fixed potential. As we noted how the amplitude of I_{max} and the value of Q varies with applied potential, the charge density measured of quantal glutamate release was also evaluated as a function of glutamate concentration and applied potential. The charge density was derived from the detected charge (Q) for the recorded single current spikes and related to the LUV volume that was determined via the measured LUV diameter using nanosized tracking analysis system (Figure 2C). We found that each potential provided its own linear calibration curve (Figure 2D, Figure S2A,B) with all being parallel to one another and differing by the calibration plot intercept, with the -0.9 V recording providing the largest and -0.5 V providing the lowest, which is in agreement with predictions according to recorded current-voltage plots for H_2O_2 (Figure S1E,F)

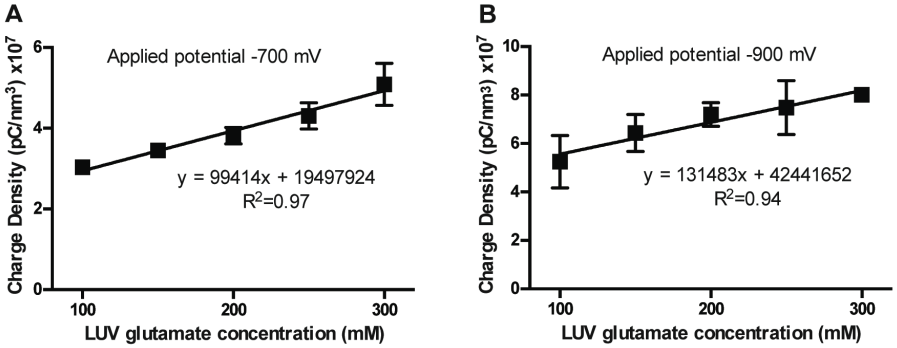

Figure S2. Calibration curve constructed from recording of LUV glutamate release at an applied potential of (A) -700 mV and (B) -900 mV vs a Ag/AgCl reference electrode. Each data point is an average of charge density from glutamate measurements of LUVs with 5 different glutamate concentration loaded into at one applied potential ± SEM.

Using the LUVs calibration for quantification of vesicle glutamate quantal size and exocytotic glutamate release

After the analysis of the current spikes recorded from glutamate release by glutamate-filled LUVs (Figure 1B), isolated synaptic vesicles (Figure 1C) and exocytotic glutamate release from brain cells in the core region of the nucleus accumbens of mouse (Figure 3A) and rat (Figure S3A) brain tissue, the kinetic and quantitative parameters were analyzed and summarized in Table S5 and S6. Here, the current spikes detected from the exocytosis recordings were divided as categorized by the different dynamic shapes as illustrated in Figure 3A). First by looking at the exocytosis measurements, it shows that the not only the frequency of the different spike types are similar in the two species, but also the temporal value of each category of spikes (i.e. $T_{1/2}$, T_{rise} and T_{fall}) as well as the quantitative measures (I_{max} and Q) are very comparable. This implies that the glutamate exocytosis events in mouse and rat brain most probably use very similar release mechanisms that result in similar vesicle quantal size released.

Besides, the current spikes detected when quantifying the glutamate content in isolated synaptic vesicles from mouse brain also present similar current spike dynamics and total current spike charge as recorded from exocytosis events in mouse brain slice. We note that glutamate release from isolated synaptic vesicles bursting, show both a faster T_{rise} and slower T_{fall} compared to what is detected in exocytosis glutamate release. The slower release kinetics at exocytosis is most likely due to the fact that the dynamics of glutamate release is controlled by the complex SNARE-mediated exocytosis machinery the regulate the formation, dilation and closure of the fusion pore that connects the vesicle compartment to the cell plasma membrane, which is an important feature in regulation of neurotransmitter release and perhaps is the factor behind the resulting different type of categories of current spikes that are detected in these recordings.

The calibration curve obtained from glutamate analysis of the glutamate-filled LUVs were then also used to determine the absolute glutamate quantities of glutamate molecules released from individual exocytosis events during spontaneous glutamate activity in the nucleus accumbens of mouse and brain tissue (Figure 3B, S3B). We noted that the amount glutamate in isolated vesicles was larger than from exocytosis release when events were detected as "sharp spikes" and that the amount was not significantly different for the other complex spike shapes recorded. This difference in quantity between the glutamate stored in isolated synaptic vesicles and the amount released, assuming minimal loss of the vesicle glutamate content at the isolation process,[13] might stem from different mechanisms of exocytosis present or that glutamate release of more than one vesicle quantal load is detected.[11,14]

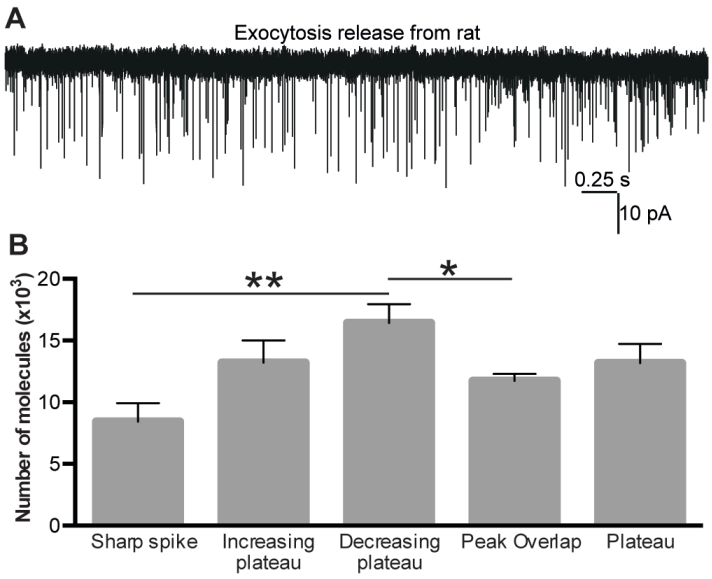

Figure S3. (A) Amperometric recording (10 kHz) of single exocytotic glutamate release in the core region of the nucleus accumbens of rat brain slice using the ultrafast glutamate sensor and applying a -0.5 V potential vs a Ag/AgCl reference electrode. (B) The number of glutamate molecules released during single exocytosis events was categorized for the different shape of single current spikes recorded. The data is presented as the average number ± SEM and with a two-tailed paired student´s t-test, *$p < 0.05$, **$p < 0.01$.

Table S3 Current spike analysis from amperometric recording of glutamate content in isolated mouse synaptic vesicles and glutamate release from single exocytosis events at the core region of the nucleus accumbens in mouse brain tissue.

		$T_{1/2}$ (ms)	T_{rise} (ms)	T_{fall} (ms)	I_{max} (pA)	Q (fC)	Spike No.
Mouse brain (n=4)	Sharp spike	0.18±0.07	0.11±0.03	0.06±0.01	9±2	1.8±0.3	427
	Increasing plateau	0.19±0.07	0.19±0.08	0.06±0.02	9.1±0.8	5±3	32
	Decreasing plateau	0.17±0.05	0.07±0.02	0.09±0.05	10±1	5±3	60
	Peak overlap	0.2±0.1	0.13±0.05	0.15±0.08	12±2	3.2±0.9	415
	Plateau	0.3±0.1	0.12±0.07	0.22±0.09	11±2	3±1	50
	Average	0.2±0.0	0.12±0.02	0.12±0.03	10±1	4±1	N/A
Synaptic vesicle (mouse, n=4)		0.16±0.01	0.08±0.01	0.14±0.01	10.9±0.8	2.2±0.1	762
LUVs (n=21)		0.68±0.04	0.31±0.01	0.56±0.08	43±4	40±5	2967

The exocytosis data is presented as the average of means ± SEM. The data from LUVs analysis is the average of averaged values for detection glutamate release from LUVs with 5 different loaded glutamate concentration.

Table S4. Current spike analysis from amperometric recording of glutamate release from single exocytosis events at the core region of the nucleus accumbens in rat brain tissue

		$T_{1/2}$ (ms)	T_{rise} (ms)	T_{fall} (ms)	I_{max} (pA)	Q (fC)	Spike No.
Rat brain (n=4)	Sharp spike	0.5±0.2	0.19±0.07	0.1±0.1	9±3	2.7± 0.4	317
	Increasing plateau	0.8±0.4	0.8±0.4	0.1±0.1	7±2	4.2±0.7	32
	Decreasing plateau	0.8±0.4	0.3±0.1	0.3±0.5	9±3	5.3±0.5	104
	Peak overlap	0.6±0.3	0.3±0.1	0.2±0.2	8±3	3.8±0.2	332
	Plateau	0.8±0.4	0.4±0.2	0.2±0.1	10±4	4.2±0.5	101
	Average	0.7±0.1	0.4±0.1	0.4±0.1	9±1	4.0±0.4	N/A

The data are shown as the means of means of spike kinetics ± SEM.

III. References

(1) Lovrić, J.; Najafinobar, N.; Dunevall, J.; Majdi, S.; Svir, I.; Oleinick, A.; Amatore, C.; Ewing, A. G. On the Mechanism of Electrochemical Vesicle Cytometry: Chromaffin Cell Vesicles and Liposomes. *Faraday Discuss.* **2016**, *193*, 65–79.

(2) Riske, K. A.; Dimova, R. Electro-Deformation and Poration of Giant Vesicles Viewed with High Temporal Resolution. *Biophys. J.* **2005**, *88* (2), 1143–1155.

(3) Tsong, T. Y. Electroporation of Cell Membranes. *Biophys. J.* **1991**, *60* (2), 297–306.

(4) Dunevall, J.; Fathali, H.; Najafinobar, N.; Lovric, J.; Wigström, J.; Cans, A.-S.; Ewing, A. G. Characterizing the Catecholamine Content of Single Mammalian Vesicles by Collision–Adsorption Events at an Electrode. *J. Am. Chem. Soc.* **2015**, *137* (13), 4344–4346.

(5) Wang, C.; Ye, F.; Velardez, G. F.; Peters, G. H.; Westh, P. Affinity of Four Polar Neurotransmitters for Lipid Bilayer Membranes. *J. Phys. Chem. B* **2011**, *115* (1), 196–203.

(6) Lipowsky, R. Bending of Membranes by Anchored Polymers. *Europhys. Lett.* **1995**, *30* (4), 197–202.

(7) Simon, J.; Kühner, M.; Ringsdorf, H.; Sackmanna, E. Polymer-Induced Shape Changes and Capping in Giant Liposomes. *Chem. Phys. Lipids* **1995**, *76* (2), 241–258.

(8) Döbereiner, H.-G.; Selchow, O.; Lipowsky, R. Spontaneous Curvature of Fluid Vesicles Induced by Trans-Bilayer Sugar Asymmetry. *Eur. Biophys. J.* **1999**, *28* (2), 174–178.

(9) Kakorin, S.; Neumann, E. Kinetics of the Electroporative Deformation of Lipid Vesicles and Biological Cells in an Electric Field. *Berichte der Bunsengesellschaft für Phys. Chemie* **1998**, *102* (4), 670–675.

(10) Reimhult, E.; Höök, F.; Kasemo, B. Intact Vesicle Adsorption and Supported Biomembrane Formation from Vesicles in Solution: Influence of Surface Chemistry, Vesicle Size, Temperature, and Osmotic Pressure †. *Langmuir* **2003**, *19* (5), 1681–1691.

(11) Wang, Y.; Mishra, D.; Bergman, J.; Keighron, J. D.; Skibicka, K. P.; Cans, A.-S. Ultrafast Glutamate Biosensor Recordings in Brain Slices Reveal Complex Single Exocytosis Transients. *ACS Chem. Neurosci.* **2019**, *10* (3), 1744–1752.

(12) Keighron, J. D.; Wigström, J.; Kurczy, M. E.; Bergman, J.; Wang, Y.; Cans, A.-S. Amperometric Detection of Single Vesicle Acetylcholine Release Events from an Artificial Cell. *ACS Chem. Neurosci.* **2015**, *6* (1), 181–188.

(13) Carlson, M. D.; Ueda, T. Accumulated Glutamate Levels in the Synaptic Vesicle Are Not Maintained in the Absence of Active Transport. *Neurosci. Lett.* **1990**, *110* (3), 325–330.

(14) Helassa, N.; Dürst, C. D.; Coates, C.; Kerruth, S.; Arif, U.; Schulze, C.; Wiegert, J. S.; Geeves, M.; Oertner, T. G.; Török, K. Ultrafast Glutamate Sensors Resolve High-Frequency Release at Schaffer Collateral Synapses. *Proc. Natl. Acad. Sci.* **2018**, *115* (21), 5594–5599.

(15) Mayer, L. D.; Hope, M. J.; Cullis, P. R.; Janoff, A. S. Solute Distributions and Trapping Efficiencies Observed in Freeze-Thawed Multilamellar Vesicles. *Biochim. Biophys. Acta - Biomembr.* **1985**, *817* (1), 193–196.

(16) Finot, M. O.; Braybrook, G. D.; Mcdermott, M. T. Characterization of Electrochemically Deposited Gold Nanocrystals on Glassy Carbon Electrodes. *J. Electroanal. Chem.* **1999**, *466* (2), 234–241.

(17) Ahmed, S.; Holt, M.; Riedel, D.; Jahn, R. Small-Scale Isolation of Synaptic Vesicles from Mammalian Brain. *Nat. Protoc.* **2013**, *8* (5), 998–1009.

(18) Budzinski, K. L.; Allen, R. W.; Fujimoto, B. S.; Kensel-Hammes, P.; Belnap, D. M.; Bajjalieh, S. M.; Chiu, D. T. Large Structural Change in Isolated Synaptic Vesicles upon Loading with Neurotransmitter. *Biophys. J.* **2009**, *97* (9), 2577–2584.

(19) Mosharov, E. V; Sulzer, D. Analysis of Exocytotic Events Recorded by Amperometry. *Nat. Methods* **2005**, *2*, 651.